AGU PUBLICATIONS

Geophysical Research Letters

RESEARCH LETTER

10.1002/2017GL076173

Key Points:

- We introduce the CO_2-forcing-equivalent metric
- Estimation of CO_2-forcing-equivalent emissions to date is presented
- Characterizing of multigas emissions scenarios and budgets in terms of CO_2-forcing-equivalent emissions is shown

Correspondence to:
S. Jenkins,
stuart.jenkins@wadham.ox.ac.uk

Citation:
Jenkins, S., Millar, R. J., Leach, N., & Allen, M. R. (2018). Framing climate goals in terms of cumulative CO_2-forcing-equivalent emissions. *Geophysical Research Letters*, *45*, 2795–2804. https://doi.org/10.1002/2017GL076173

Received 27 OCT 2017
Accepted 20 FEB 2018
Accepted article online 27 FEB 2018
Published online 26 MAR 2018

Framing Climate Goals in Terms of Cumulative CO_2-Forcing-Equivalent Emissions

S. Jenkins[1,2], R. J. Millar[2,3], N. Leach[1,2], and M. R. Allen[1,2]

[1]Department of Physics, University of Oxford, Oxford, UK, [2]Environmental Change Institute, University of Oxford, Oxford, UK, [3]College of Engineering, Mathematical and Physical Sciences, University of Exeter, Exeter, UK

Abstract The relationship between cumulative CO_2 emissions and CO_2-induced warming is determined by the Transient Climate Response to Emissions (TCRE), but total anthropogenic warming also depends on non-CO_2 forcing, complicating the interpretation of emissions budgets based on CO_2 alone. An alternative is to frame emissions budgets in terms of CO_2-forcing-equivalent (CO_2-fe) emissions—the CO_2 emissions that would yield a given total anthropogenic radiative forcing pathway. Unlike conventional "CO_2-equivalent" emissions, these are directly related to warming by the TCRE and need to fall to zero to stabilize warming: hence, CO_2-fe emissions generalize the concept of a cumulative carbon budget to multigas scenarios. Cumulative CO_2-fe emissions from 1870 to 2015 inclusive are found to be 2,900 ± 600 $GtCO_2$-fe, increasing at a rate of 67 ± 9.5 $GtCO_2$-fe/yr. A TCRE range of 0.8–2.5°C per 1,000 GtC implies a total budget for 0.6°C of additional warming above the present decade of 880–2,750 $GtCO_2$-fe, with 1,290 $GtCO_2$-fe implied by the Coupled Model Intercomparison Project Phase 5 median response, corresponding to 19 years' CO_2-fe emissions at the current rate.

Plain Language Summary The relationship between the global average temperature anomaly (the difference between the global average current temperature and the global average preindustrial temperature) and the total quantity of CO_2 emissions released is linear. However, contributions from other greenhouse gases mean that this simple relationship is lost. We propose a new way of comparing greenhouse gases by converting them into a "forcing equivalent" quantity of CO_2. This method means that the linear relationship between total CO_2-forcing-equivalent (CO_2-fe) emissions and warming remains linear. This new greenhouse gas metric allows us to estimate the total CO_2-forcing-equivalent emissions released over the industrialized period (1870–2015) as 2,900 ± 600 $GtCO_2$-fe, and increasing at a rate of 67 ± 9.5 $GtCO_2$-fe/yr. Budgets of remaining CO_2-forcing-equivalent emissions to key temperature stabilization goals are also estimated, showing that the CO_2-fe emissions metric is a useful way to characterize budgets to key temperature stabilization goals when considering multigas mitigation pathways.

1. Introduction

Understanding the contributions of different greenhouse gases and other climate forcing agents to global temperature change is important for assessing their implications of mitigation pathways and goals. The Intergovernmental Panel on Climate Change Fifth Assessment Report, or AR5 (Stocker et al., 2013), introduced the concept of a cumulative carbon budget, based on the work of Forster et al. (2007), Meinshausen et al. (2009), Allen et al. (2009), and Matthews et al. (2009). This exploits the monotonic, near-linear, scenario-independent relationship between cumulative CO_2 emissions and CO_2-induced warming to compare the implications of different emissions scenarios for the risks of warming in the range of 2–5°C. For higher warming levels, global temperature change is dominated by CO_2, so the Transient Climate Response to (cumulative CO_2) Emissions (TCRE), defined as the warming response to the emission of one trillion tonnes of carbon (1 TtC, or 3.67 trillion tonnes of CO_2), multiplied by cumulative CO_2 emissions, provides a useful indication of the minimum warming expected under any specific emissions scenario, assuming (as in all current scenarios) the net overall impact of non-CO_2 climate forcing is positive around the time of peak warming. The larger the contribution of non-CO_2 climate forcing agents, the lower the policy relevance of CO_2-induced warming determined by the TCRE. This is particularly an issue for more ambitious mitigation scenarios, such as "pursuing efforts" to hold warming from preindustrial to below 1.5°C, one of the ambitions of the Paris Climate Agreement (Rogelj et al., 2016; United Nations Framework Convention on Climate Change, 2015).

One approach to this problem (e.g., Millar, Fuglestvedt, et al., 2017) is to specify non-CO_2 climate forcing based on a particular emissions scenario, and diagnose allowable CO_2 emissions as a residual. Another (e.g., Meinshausen et al., 2009; Stocker et al., 2013, Figure SPM10; Rogelj et al., 2016) is to consider a range of scenarios and exploit the emergent, scenario-dependent relationship between cumulative CO_2 emissions and non-CO_2 climate forcing to assess the total anthropogenic warming expected for a given level of cumulative CO_2 emissions. Both approaches are open to the criticism that they potentially obscure the relative importance of non-CO_2 forcing, either by not allowing it to vary at all or by assuming that it varies approximately in proportion to CO_2 forcing with the ratio determined by the scenarios that happen to be available.

Conventional methods of expressing total anthropogenic emissions as "CO_2 equivalent" using a metric such as the global warming potential (Shine et al., 2005) should not be used to quantify contributions of short-lived climate pollutants (SLCPs) to cumulative emission budgets, because SLCPs do not accumulate in the climate system (Shine et al., 2005). Variations on global warming potentials have been proposed (Allen et al., 2016; Lauder et al., 2013) to address this, but these depend on metric values that still depend on relatively arbitrary choices, such as the binary distinction between "long-lived" and "short-lived" climate pollutants in Allen et al. (2016).

A more direct approach, building on the notion of a forcing equivalent index proposed by Wigley (1998) and elaborated in Manning and Reisinger (2011), is to express net total anthropogenic radiative forcing in terms of CO_2-forcing-equivalent (CO_2-fe) emissions, defined simply as the time history of CO_2 emissions that would result in a given radiative forcing pathway (similar to the approach of Zickfeld et al. (2009), who go a step farther and diagnose anthropogenic radiative forcing from temperatures). A carbon cycle model is required to compute CO_2-fe emissions, but since the relationship between radiative forcing and CO_2-equivalent concentrations is relatively unambiguous, and CO_2 emissions are diagnosed from CO_2 concentrations in many climate modeling experiments already (Friedlingstein et al., 2006), calculating CO_2-fe emissions in this way is no more model dependent than calculating CO_2 emissions themselves.

Figure 1 shows a schematic example of the concept of CO_2-fe emissions. Panel (a) contains two idealized radiative forcing scenarios (dotted and solid lines), with the same total forcing (red) but where different proportions are from CO_2 (black) and non-CO_2 (blue) sources after 2020: dotted lines show a scenario in which non-CO_2 forcing continues to increase, while solid lines show a scenario in which it is stabilized. Panel (b) shows the corresponding CO_2-fe emissions for each scenario: note that increasing non-CO_2 forcing equates to approximately steady CO_2-fe emissions, mimicking the cumulative impact of CO_2, while stabilizing non-CO_2 forcing equates to an immediate decrease of CO_2-fe emissions toward zero. The total CO_2-fe emissions are identical except for smoothing errors and small nonlinearities from the calculation method. Temperature responses to these two scenarios would also be identical, and diamond symbols show the year in which temperatures stabilize. Unlike CO_2 emissions alone, CO_2-fe emissions reaching net zero is an accurate and scenario-independent indicator of "emissions balance" if interpreted in terms of the conditions required for temperature stabilization (Fuglestvedt et al., 2018).

Defined in this way, rapidly falling SLCP emissions correspond to negative CO_2-fe emissions, since both act to reduce radiative forcing. Very rapid changes in SLCP emissions correspond to large-amplitude "spikes" (positive or negative) in CO_2-fe emissions, making them difficult to interpret. Hence, the concept of CO_2-fe emissions is best applied to scenarios where non-CO_2 forcing agents are varying relatively slowly. It is, however, still more general than CO_2-equivalent emissions defined with traditional metrics. Revisions to forcing, such as Etminan et al. (2016), change metric values but would also change the CO_2-fe emissions introduced here. In this paper, we diagnose CO_2-fe emissions using the Finite Amplitude Impulse Response (FAIR) model defined by Millar, Nicholls, et al. (2017), which is based on the AR5 impulse response model (Joos et al., 2013; Myhre et al., 2013) but allows impulse response time scales to vary with global temperature and carbon uptake to mimic the behavior of more complex carbon cycle models. Details of the calculation are given in the following section.

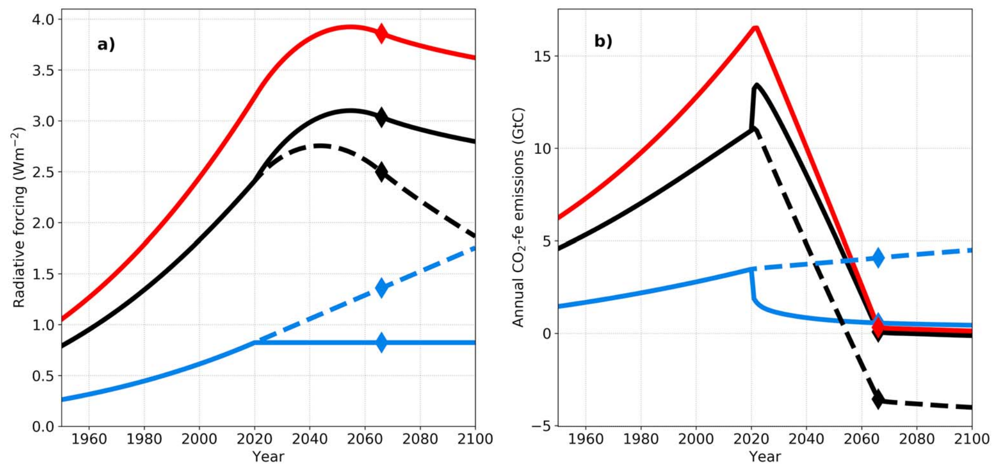

Figure 1. Two idealized radiative forcing profiles (a) solid and dotted lines) are split so that their total radiative forcing is identical (red), but with different proportions arising from CO_2 (black) and non-CO_2 (blue) sources after 2020. Panel (b) shows these scenarios expressed in terms of CO_2-fe emissions. Since the total forcing is identical, the diagnosed total CO_2-fe emissions are the same, but with different contributions coming from CO_2 and non-CO_2 sources in each case. The temperature response to these total CO_2-fe emissions pathways would be identical, assuming non-CO_2 forcings have been accurately expressed in terms of effective radiative forcing. Diamond symbols show the year of temperature stabilization.

2. Diagnosing CO_2-Forcing-Equivalent Emissions Using the FAIR Model

Following Joos et al. (2013), the FAIR model represents the evolution of the atmospheric CO_2 concentrations (in ppm) C from a preindustrial equilibrium value C_0 using four carbon reservoirs

$$\frac{\mathrm{d}R_i}{\mathrm{d}t} = a_i E - \frac{R_i}{\alpha\tau_i}\,; \quad C = C_0 + \sum_i R_i\,; \quad i = 1-4\,, \tag{1}$$

where E are annual emissions (in GtC), R_i may be thought of as the anomalous concentration in the ith reservoir, the a_i are four coefficients that sum to 0.47 ppm/GtC, and the τ_i are time constants, one of which is infinite. The only novel element in FAIR is the coefficient α, a state-dependent scaling factor that depends on the 100 year integrated Impulse-Response Function (iIRF_{100}), which is modeled as a simple linear function of global mean surface temperature, T, and carbon accumulated in the oceans and biosphere $C_{\mathrm{acc}} = \sum_t E - (C - C_0)$:

$$\mathrm{iIRF}_{100} = \sum_i \alpha a_i \tau_i \left[1 - \exp\left(\frac{-100}{\alpha\tau_i}\right)\right] = \gamma\left[r_0 + \beta(r_C C_{\mathrm{acc}} + r_T T)\right]\,, \tag{2}$$

In the calculations presented here, T is diagnosed from observations or from more complex models, so no use is made of the FAIR thermal-response model.

Forcing-equivalent emissions are computed by first calculating equivalent CO_2 concentrations from radiative forcing F

$$C = C_0 \exp\left(\frac{F\,\ln(2)}{F_{2\mathrm{x}}}\right) \tag{3}$$

and then diagnosing the value of E at each time step that reproduces the desired value of C. Diagnosed emissions are subject to two-time-step noise which we remove with a Gaussian kernel ($\sigma = 5$ years). All parameters are as given in Myhre et al. (2013) and Millar, Nicholls, et al. (2017), with the exception of β and γ, which are estimated from Coupled Model Intercomparison Project Phase 5 (CMIP5) models (in section 3) or from Global Carbon Project (GCP) observations (in section 4).

3. Application to CMIP5 Earth System Model Ensemble

We first demonstrate the calculation of CO_2-fe emissions on the CMIP5 Earth System Model (ESM) ensemble (Arora et al., 2013) to assess its robustness before applying to observations. Figure 2a shows atmospheric CO_2 concentrations plotted against cumulative CO_2 emissions in three ESM ensembles: the 1% per year increasing

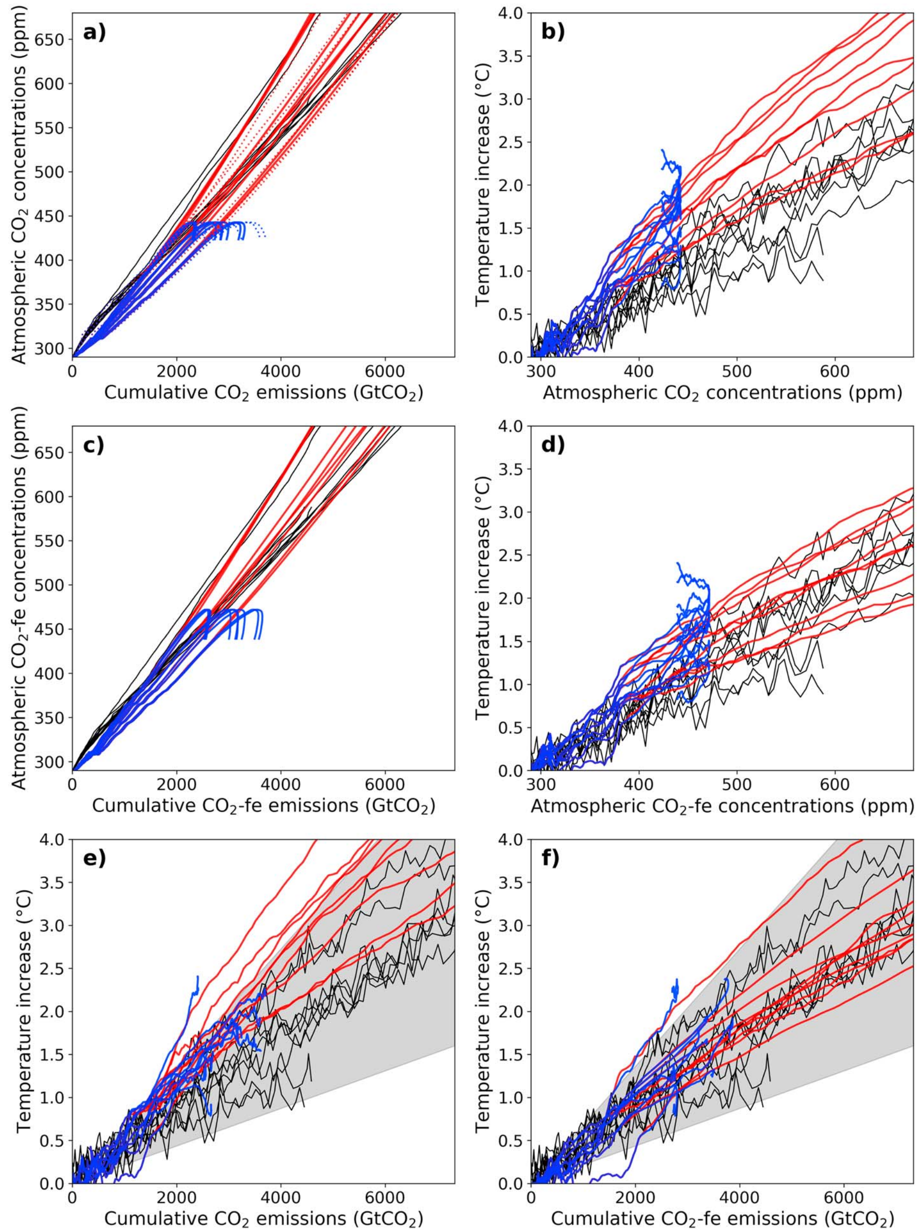

Figure 2. Panel (a) shows CO_2 concentrations plotted against cumulative CO_2 emissions for models included in the Coupled Model Intercomparison Project Phase 5 Earth System Model (ESM) ensemble. The 1%/yr CO_2 concentration increase experiment is shown in black, Representative Concentration Pathway 2.6 (RCP2.6) in blue and RCP8.5 in red. Dotted lines show diagnosed CO_2 emissions from the ESMs' own carbon cycle model, solid lines are Finite Amplitude Impulse Response (FAIR)-diagnosed CO_2 emissions. Panel (b) shows ESM temperature responses against CO_2 concentrations for the 1% (black), RCP2.6 (blue), and RCP8.5 (red) scenarios in panel (a). In panel (c) the same Coupled Model Intercomparison Project Phase 5 models concentration time series are now plotted against FAIR-diagnosed CO_2-fe emissions from the total effective radiative forcing using a parameter set chosen to mimic each ESM. Panel (d) shows the ESM temperature responses plotted against the atmospheric CO_2-fe concentration. Panel (e) plots ESM temperature responses plotted against FAIR-diagnosed cumulative CO_2 emissions. Panel (f) shows the same ESM temperature responses as in panel (e), now plotted against cumulative CO_2-fe emissions calculated from the total effective radiative forcing.

CO_2 concentration scenario in black, historical, and Representative Concentration Pathway 8.5 (RCP8.5) scenario in red, and historical and RCP2.6 scenario in blue. Dashed lines show cumulative CO_2 emissions diagnosed from the ESMs' own carbon cycle models, while solid lines show emissions diagnosed using the FAIR model running from 1850 to 2100 with $C_0 = 290$ ppm to mimic the CMIP design. CO_2 emissions are also diagnosed directly from the ESMs in the (concentration driven) 1% per year increasing CO_2 simulations. The parameters β and γ are fitted to each ESM by minimizing the sum squared residual cumulative diagnosed emissions for the historical and RCP8.5 simulations over the period 1865–2095 for which the relevant CMIP5 outputs are available. The similarity of the solid and dotted lines indicates that this relatively simple carbon cycle model is adequate to capture key features of the global behavior of the members of the CMIP5 model ensemble adjusting only two parameters. The increase in airborne fraction (upward curvature) evident in the 1% and RCP8.5 simulations, and the reduction and reversal under RCP2.6, are both reproduced. Panel (b) shows temperatures in the CMIP5 ESM ensemble plotted against atmospheric CO_2 concentrations. There is a clear offset between the RCP ensembles and the 1% per year CO_2-only ensemble due to non-CO_2 climate drivers.

Figure 2c shows the same ESM models in red and blue, plotting atmospheric CO_2-fe concentrations computed from total effective radiative forcing (ERF) in the individual CMIP5 ESM integrations (Forster et al., 2013) using equation (3) with $C_0 = 290$ ppm, plotted against cumulative CO_2-fe emissions diagnosed with the FAIR model, using the same combination of β and γ for each ESM as in panel (a). These follow the same relationship as the CO_2 emissions alone in panel (a), with the differences coming from the extra contribution from non-CO_2 forcing. For example, this means that CO_2-fe concentrations in RCP2.6 peak at a higher level.

Figure 2d shows the ESM-calculated temperatures plotted against atmospheric CO_2-fe concentrations. The offset between the RCP8.5 ensemble and the 1% ensemble is largely resolved, as expected since CO_2-fe concentrations scale with total radiative forcing, and the temperature response to ERF is, by design, independent of the forcing agent. The correspondence is not perfect, and the bias is at its largest at around present-day forcing (around 450 ppm CO_2-fe) when the fractional contribution of non-CO_2 climate forcing agents to total anthropogenic forcing is at its largest. An additional reason for differences later in the century is that the temperature response is dependent on the history of forcing, not just the instantaneous forcing level (Gregory et al., 2015). Nevertheless, to a good approximation, the realized warming at a given level of total forcing (and hence at a given CO_2-fe equivalent concentration) seems largely forcing independent, provided efficacies of different forcings are correctly accounted for (Shindell, 2014).

Figure 2e shows the familiar plot of temperatures in the CMIP5 ensembles plotted against cumulative CO_2 emissions, with the gray region showing the Intergovernmental Panel on Climate Change AR5 assessed range for the TCRE of 0.8–2.5°C per 1,000 GtC. The offset between RCP and CO_2-only ensembles is clearly evident, such that the standard TCRE is clearly not an adequate metric for predicting total anthropogenic warming per tonne of CO_2 emitted in the presence of multiple forcing agents. In contrast, panel (f) shows the same temperatures plotted against cumulative CO_2-fe emissions computed from total radiative forcing as in the lines in panel (c). Since it is now a like-for-like comparison, the response to CO_2-fe emissions is very similar to the response to the same quantity of pure CO_2 emissions, so the TCRE can be applied to both. Using CO_2-fe provides agreement in the ratio of warming to cumulative CO_2-fe emissions over different multigas scenarios in the CMIP5 model ensemble. Since the TCRE can be constrained by multiple lines of evidence (Gillett et al., 2013), this shifts the focus of carbon budget calculations to resolving uncertainty in the TCRE and the question of quantifying CO_2-fe emissions to date, discussed in the following section.

4. Diagnosing CO_2 Emissions to Date

In order to diagnose CO_2-fe emissions for the past we must have an accurate representation of the evolution of the global airborne fraction over the industrialized period. We first diagnose CO_2 emissions in the period 1870–2015 from estimated CO_2 radiative forcing time series (Myhre et al., 2013) and compare the annual budget in 2015 and the cumulative budget for the period 1870–2015 with observed estimates and uncertainties, from the GCP (Le Quéré et al., 2016). In order to do this we first use the median CO_2 radiative forcing data to find a compatible CO_2 concentration profile, via equation (3). We then use the FAIR model run over a range of parameter sets (generated by varying β and γ independently in equation (2) to diagnose CO_2 emissions time series, which are compatible with this CO_2 concentration profile and temperature response. We use these values to test the uncertainty in our model due to uncertainty in FAIR's carbon cycle parameters

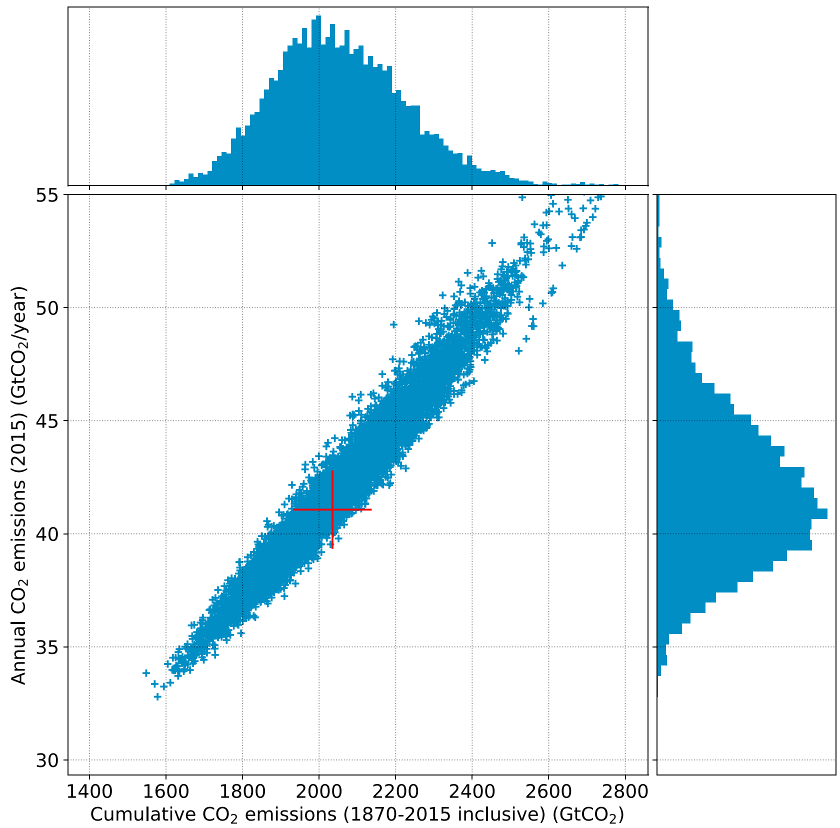

Figure 3. Distribution of cumulative CO_2 emissions (1870–2015) (top histogram) and annual CO_2 emissions in 2015 (right histogram) calculated using 10,000 Monte Carlo sampled parameter sets (blue crosses). Red cross is the Global Carbon Project best estimate value of cumulative and annual CO_2 emissions.

and to define a best estimate parameter set with which we can accurately reproduce the mean and spread of the CO_2 emissions and radiative forcing data.

Observations of global quantities alone are insufficient to constrain all three parameters r_0, r_C, and r_T, so we fix the ratio r_T/r_C to the value given in Millar, Nicholls, et al. (2017), which in turn was based on the experiments presented in Gregory et al. (2009) and Arora et al. (2013). For relatively small warming levels and scenarios of monotonically increasing emissions, results are insensitive to this ratio, because both r_T and r_C have a similar impact on the evolution of airborne fraction. Varying β and γ independently is equivalent to assuming that uncertainty in the overall strength of carbon sinks over the industrialized period (denoted by γ) is independent of the fractional rate at which these sinks are changing due to rising temperatures and accumulating carbon (denoted by β). While this assumption is debatable, it seems preferable to varying r_0 and the combination of r_T and r_C independently. To diagnose emissions we require a temperature profile T. We use observational data from the HadCRUT4 data set (Morice et al., 2012), smoothed with a Gaussian kernel ($\sigma = 5$ years). The temperature anomaly is adjusted to have an average value of 0.1°C in the period 1850–1879, consistent with Schurer et al. (2017). We use a linear ramp to connect the zero temperature anomaly in 1750 to its value in 1850. Since carbon cycle parameters are fitted to the observed airborne fraction, and the impact of carbon cycle feedbacks is relatively small over the historical period, the choice of temperature data set has very little impact on results.

We randomly sample β and γ values (defined in equation (2) for estimating $iIRF_{100}$) and diagnose CO_2 emissions time series using the FAIR model and the time series of historical CO_2 forcing from Forster et al. and identify the region of the parameter space that generates cumulative emissions to date and current emission rates within the uncertainty range quoted in the GCP (Le Quéré et al., 2016). We find that varying each parameter independently is associated with moving the derived ellipse of emissions (as plotted in Figure 3) along a line in the space, so we find a single combination of β and γ parameters that best fit the GCP data.

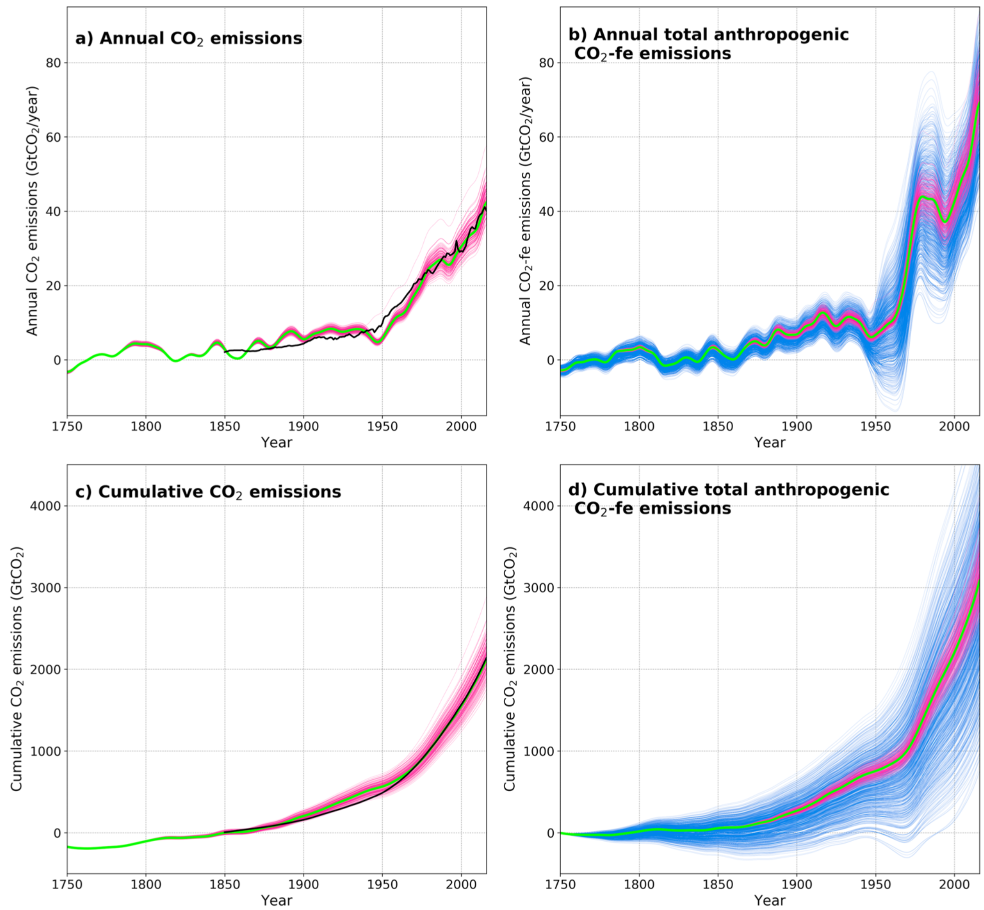

Figure 4. Diagnosed CO_2-fe emissions using temperature and radiative forcing (RF), accounting for uncertainty in observations and response. (a) Diagnosed annual CO_2 emissions using the Finite Amplitude Impulse Response model with best estimate parameters and forcing (green), and with ensemble of 200 parameter sets (pink). The black line shows annual CO_2 emissions data from the Global Carbon Project (GCP). (b) Diagnosed annual CO_2-fe emissions for the ensemble of 200 realizations of total anthropogenic RF, each computed with 200 parameter sets to provide combined uncertainty of both model and forcing (blue). Pink shows best estimate RF with 200 parameter sets, showing impact of model uncertainty. CO_2-fe emissions calculated with best estimate total anthropogenic RF and best parameter set shown in green. (c) Cumulative CO_2 emissions from the diagnosed annual CO_2 emissions in panel (a) (ensemble in pink; best estimate in green). Black shows cumulative GCP emissions. (d) Cumulative CO_2-fe emissions for the diagnosed CO_2-fe emissions in panel (b) (forcing and response uncertainty in blue; response uncertainty alone in pink; and best estimate in green).

The quoted GCP emissions values are 2035 ± 202 $GtCO_2$ (555 ± 55 GtC) released in the period 1870–2015 with 41 ± 2.6 $GtCO_2$ (11.2 ± 0.7 GtC) released in 2015.

To find the uncertainty range, we use the 5–95% confidence intervals to set the standard deviations of β and γ, and to avoid results being too sensitive to emissions in a single year, and constrain the current airborne fraction to be consistent with recent estimates (Knorr, 2009). Best estimate values of $\gamma = 1.07$ (± 0.10) and $\beta = 0.70$ (± 0.19), corresponding to the notation of Millar, Nicholls, et al. (2017) to values of $r_0 = 34.67$ (± 3.24) year, $r_C = 0.0142$ (± 0.0038) year GtC^{-1} and $r_T = 3.120$ (± 0.833) year K^{-1}, yield cumulative 1870–2015 CO_2 emissions of 2025 ± 177 $GtCO_2$ (552 ± 48.3 GtC; 1984 $GtCO_2$ to 2014 end), with 40.5 ± 3.5 $GtCO_2$/yr (11.1 ± 0.95 GtC/yr) released in 2015 and a current airborne fraction of 42% (± 3.5%), in good agreement with published values. The joint distribution of cumulative emissions to date and emissions in 2015 from a random independent sampling of β and γ is shown in Figure 3, while diagnosed emissions corresponding to the best estimate CO_2 radiative forcing time series are compared with observed GCP emissions in Figure 4a.

Total anthropogenic ERF is obtained following the procedure of Myhre et al. (2013), with updated estimates of methane forcing (Etminan et al., 2016). In Figure 4 forcing uncertainty is expressed by a sample of 200 equiprobable time series. These are combined with 200 (β, γ) combinations to diagnose 40,000 possible time series of CO_2-fe emissions corresponding to total historical anthropogenic radiative forcing. Samples of 200 using only the best estimate radiative forcing are shown in pink, to illustrate the impact of carbon cycle uncertainty, while samples in blue show the combined impact of carbon cycle and radiative forcing uncertainty. It is clear that radiative forcing uncertainty, primarily from non-CO_2 forcing agents, dominates, with uncertainty in the carbon cycle model playing a relatively minor role. Hence, CO_2-fe emissions represent a relatively unambiguous method of characterizing the evolution of total anthropogenic influence on climate. We find cumulative CO_2-fe emissions for the period 1870–2015 of 2900 ± 600 $GtCO_2$-fe (790 ± 164 GtC-fe; 2832 ± 599 $GtCO_2$-fe released in period 1870–2014), with annual emissions in 2015 of 67 ± 9.5 $GtCO_2$-fe/yr (18.1 ± 2.6 GtC-fe/yr). CO_2-fe emission rates in 2014 are found to be 64 ± 10.2 $GtCO_2$-fe (17.5 ± 2.8 GtC-fe).

One remaining carbon cycle parameter that can add uncertainty to the model is the preindustrial CO_2 concentration value, C_0. We use a standard value of 278 ppm. Calculating the cumulative CO_2-fe emissions for the 1870–2015 period with variations in preindustrial CO_2 concentration of ±3 ppm, we find variations in cumulative carbon of ±29 $GtCO_2$-fe, but this is distinct from carbon cycle model uncertainty, because radiative forcing can be defined relative to a given value of C_0 in the specification of CO_2-fe.

5. Implications for Outstanding CO_2-Forcing-Equivalent Budgets

We have demonstrated in Figure 2 that cumulative CO_2-forcing-equivalent emissions represent a relatively unambiguous indicator of warming, with the constant of proportionality provided by the TCRE. This is not surprising, since CO_2-fe emissions provide, by construction, an identical ERF time series to the corresponding CO_2 emissions, so provided the temperature response to ERF is forcing independent (which is approximately true), we should expect the temperature response to be identical, and it has long been argued that the proportionality of temperatures and cumulative CO_2 emissions is scenario independent (Allen et al., 2009; Meinshausen et al., 2009; Solomon et al., 2009). The temperature responses to different forcings will be further explored by Precipitation Driver Response Model Intercomparison Project. (Center for International Climate Research (CICERO), 2013)

The AR5 assessed range for TCRE of 0.8–2.5°C per 1,000 GtC implies CO_2-fe budgets for 1.5 and 2°C of warming of 2,200–6,875 and 2,930–9,170 $GtCO_2$-fe (600–1,875 and 800–2,500 GtC-fe), respectively, but simply subtracting CO_2-fe emissions to date would exaggerate the uncertainty in outstanding budgets because uncertainties in past and future ERF are strongly correlated. The more policy-relevant range is the CO_2-fe budget for a further 0.6°C of warming above the present decade (2010–2019), which Millar, Fuglestvedt et al., (2017) suggest could be interpreted as representative of 1.5°C above preindustrial, depending on the metric used for global mean surface temperature and the choice of preindustrial reference period. The AR5 TCRE range implies a CO_2-fe budget for 0.6°C of 880–2,750 $GtCO_2$-fe (240–750 GtC-fe), while the CMIP5 ensemble median TCRE (which happens to be close to the ensemble 66th percentile because of clustering of ensemble members around this value) of 1.7°C per 1,000 GtC implies a 0.6°C budget of 1,290 $GtCO_2$-fe (350 GtC-fe). This would imply that limiting future warming to 0.6°C requires reducing CO_2-fe emissions in a straight line to zero by 2055, consistent with the conclusions of Millar, Fuglestvedt, et al. (2017) regarding CO_2 emissions alone. For limiting warming to 2°C the AR5 TCRE range implies a CO_2-fe budget of 1,614–5,042 $GtCO_2$-fe (440–1,375 GtC-fe), while the CMIP5 ensemble median TCRE implies a budget of 2,373 $GtCO_2$-fe (647 GtC-fe).

This median budget is only 15% higher than the median CMIP5-based budget for CO_2 emissions alone reported in Millar, Fuglestvedt, et al. (2017), reflecting the relatively small net contribution of non-CO_2 forcing to future warming in the modified RCP2.6 scenario used in that study. The assumption of a fixed (and relatively low) level of future non-CO_2 forcing was highlighted by Millar, Fuglestvedt, et al. (2017) as an important caveat: reformulating carbon budgets using CO_2-fe would allow the implications of both CO_2 and non-CO_2 radiative forcing agents to be made clear. The CO_2-fe budget and the current CO_2-fe emissions rate imply a similar time to net zero CO_2-fe emissions as Millar, Fuglestvedt, et al. (2017) found for CO_2 emissions. This did not have to be the case: Millar, Fuglestvedt, et al. (2017) is a residual budget (i.e., it assumes a non-CO_2 forcing contribution and then finds the remaining CO_2 contribution consistent with a given level of warming), but it so happens that the contribution of non-CO_2 agents to total anthropogenic forcing falls to zero over roughly the same time frame as CO_2 forcing (this may be different in other scenarios).

The ratio of human-induced warming to date and CO_2-fe emissions to date might be used to estimate an "observational" estimate of TCRE, but the comparison of two derived quantities is likely to be less accurate than the direct comparison of models with observations, combined with physically based scaling arguments to relate directly observable quantities to the TCRE, as in Gillett et al. (2013). Hence, we would argue that the most appropriate use of cumulative CO_2-fe emissions is to relate scenarios to budgets based on assessed ranges for the TCRE based on multiple lines of evidence. The concept of CO_2-fe emissions can in this way be used to generalize the concept of a cumulative carbon budget to multigas scenarios. It would be possible to compute CO_2-fe budgets for a range of scenarios and hence provide an objective way of comparing them that is directly relevant to their temperature response (more so than CO_2-equivalent budgets from conventional metrics, Fuglestvedt et al., 2018). For example, the two schematic CO_2-fe emissions scenarios depicted in Figure 1 are designed with total CO_2-fe budgets of 1,290 $GtCO_2$-fe. In the case of rising non-CO_2 CO_2-fe emissions (e.g., caused by reducing aerosol emissions), it is clear that CO_2 emissions must be reduced to compensate for these non-CO_2 forcing changes if the same total CO_2-fe budget and hence the same temperature outcome, is to be achieved.

A key caveat in this study is the reliance on a single simple carbon cycle model to derive CO_2-fe emissions, albeit allowing for uncertainty in model parameters. Even though the FAIR model is capable of reproducing the behavior of more complex models, as indicated in Figure 2, use of a single model structure may underestimate uncertainty. Future CMIP experiments with ESMs may wish to consider diagnosing CO_2-fe emissions from total anthropogenic ERF along with anthropogenic CO_2 emissions using the ESMs' own carbon cycle models.

Acknowledgments
We are grateful to Piers Forster and Joeri Rogelj for providing radiative forcing time series and CMIP5 AOGCM output, respectively, and Oliver Braddy, Euan Graham, and Zebedee Nicholls for assistance in developing the distribution version of the FAIR model. S. J. and N. L. were supported by the NERC, MOAP, and ECI summer placement schemes. R. J. M. was supported by the UK Natural Environment Research Council project NE/P014844/1, the ECI and the Oxford Martin School. The 200 radiative forcings data set provided by Piers Forster is available on http://www.globalwarmingindex.org/AWI/info_page.html under the hyperlink attached to "forcing" in the first paragraph below the main figure. The HADCRUT4 temperature data set is available from https://www.metoffice.gov.uk/hadobs/hadcrut4/, and the CMIP5 model ensemble data set is available from https://cmip.llnl.gov/index.html. We acknowledge the World Climate Research Programme's Working Group on Coupled Modelling, which is responsible for CMIP, and we thank the climate modeling groups for producing and making available their model output. We would also like to thank two anonymous reviewers for helpful suggestions, including the schematic Figure 1.

References

Allen, M. R., Frame, D. J., Huntingford, C., Jones, C. D., Lowe, J. A., Meinshausen, M., et al. (2009). Warming caused by cumulative carbon emissions towards the trillionth tonne. *Nature*, *458*, 1163–1166.

Allen, M. R., Fuglestvedt, J. S., Shine, K. P., Reisinger, A., Pierrehumbert, R. T., & Forster, P. M. (2016). New use of global warming potentials to compare cumulative and short-lived climate pollutants. *Nature Climate Change*, *6*, 773–776.

Arora, V. K., Boer, G. J., Friedlingstein, P., Eby, M., Jones, C. D., Christian, J. R., et al. (2013). Carbon-concentration and carbon-climate feedbacks in CMIP5 Earth system models. *Journal of Climate*, *26*, 5289–5314.

Center for International Climate Research (CICERO) (2013). Precipitation Driver Response Model Intercomparison Project (PDRMIP). https://www.cicero.uio.no/en/PDRMIP

Etminan, M., Myhre, G., Highwood, E. J., & Shine, K. P. (2016). Radiative forcing of carbon dioxide, methane, and nitrous oxide: A significant revision of the methane radiative forcing. *Geophysical Research Letters*, *43*, 12,614–12,623. https://doi.org/10.1002/2016GL071930

Forster, P. M., Andrews, T., Good, P., Gregory, J. M., Jackson, L. S., & Zelinka, M. (2013). Evaluating adjusted forcing and model spread for historical and future scenarios in the CMIP5 generation of climate models. *Journal of Geophysical Research: Atmospheres*, *118*, 2169–8996. https://doi.org/10.1002/jgrd.50174

Forster, P. M., Ramaswamy, V., Artaxo, P., Berntsen, T., Betts, R., Fahey, D. W., et al. (2007). Changes in atmospheric constituents and in radiative forcing. In S. Solomon, et al. (Eds.), *Climate change 2007: The physical science basis. Contribution of Working Group I to the Fourth Assessment Report of the Intergovernmental Panel on Climate Change*. Cambridge, United Kingdom and New York, NY, USA: Cambridge University Press.

Friedlingstein, P., Cox, P., Betts, R., Bopp, L., von Bloh, W., Brovkin, V., et al. (2006). Climate-carbon cycle feedback analysis: Results from the C4MIP model intercomparison. *Journal of Climate*, *19*, 3337–3353.

Fuglestvedt, J., Rogelj, J., Millar, R. J., Allen, M., Boucher, O., Cain, M., et al. (2018). Implications of possible interpretations of "greenhouse gas balance" in the Paris Agreement. *Philosophical Transactions of the Royal Society A*. https://doi.org/10.1098/rsta.2016.0445

Gillett, N. P., Arora, V. K., Matthews, H. D., & Allen, M. R. (2013). Constraining the ratio of global warming to cumulative CO_2 emissions using $CMIP_5$ simulations. *Journal of Climate*, *26*, 6844–6858. https://doi.org/10.1175/JCLI-D-12-00476.1

Gregory, J. M., Andrews, T., & Good, P. (2015). The inconstancy of the transient climate response parameter under increasing CO_2. *Philosophical Transactions of the Royal Society A: Mathematical, Physical and Engineering Sciences*, *373*, 20140417. https://doi.org/10.1098/rsta.2014.0417

Gregory, J. M., Jones, C., Cadule, P., & Friedlingstein, P. (2009). Quantifying carbon cycle feedbacks. *Journal of Climate*, *22*, 5232–5250.

Joos, F., Roth, R., Fuglestvedt, J. S., Peters, G. P., Enting, I. G., von Bloh, W., et al. (2013). Carbon dioxide and climate impulse response functions for the computation of greenhouse gas metrics: A multi-model analysis. *Atmospheric Chemistry and Physics*, *13*, 2793–2825.

Knorr, W. (2009). Is the airborne fraction of anthropogenic CO_2 emissions increasing? *Geophysical Research Letters*, *36*, L21710. https://doi.org/10.1029/2009GL040613

Lauder, A. R., Enting, I. G., Carter, J. O., Clisby, N., Cowie, A. L., Henry, B. K., et al. (2013). Offsetting methane emissions — An alternative to emission equivalence metrics. *International Journal of Greenhouse Gas Control*, *12*, 419–429.

Le Quéré, C., Andrew, R. M., Canadell, J. G., Sitch, S., Korsbakken, J. I., Peters, G. P., et al. (2016). Global carbon budget 2016. *Earth System Science Data*, *8*, 605–649.

Manning, M., & Reisinger, A. (2011). Broader perspectives for comparing different greenhouse gases. *Philosophical Transactions of the Royal Society A*, *369*, 1891–1905.

Matthews, H. D., Gillett, N. P., Stott, P. A., & Zickfeld, K. (2009). The proportionality of global warming to cumulative carbon emissions. *Nature*, *459*, 829–832.

Meinshausen, M., Meinshausen, N., Hare, W., Raper, S. C. B., Frieler, K., Knutti, R., et al. (2009). Greenhouse-gas emission targets for limiting global warming to 2°C. *Nature*, *458*, 1158–1162.

Millar, R. J., Fuglestvedt, J., Friedlingstein, P., Rogelj, J., Grubb, M. J., Matthews, H. D., et al. (2017). Emission budgets and pathways consistent with limiting warming to 1.5°C. *Nature Geoscience*, *10*, 741–747.

Millar, R. J., Nicholls, Z. R., Friedlingstein, P., & Allen, M. R. (2017). A modified impulse-response representation of the global near-surface air temperature and atmospheric concentration response to carbon dioxide emissions. *Atmospheric Chemistry and Physics*, *17*, 7213–7228.

Morice, C. P., Kennedy, J. J., Rayner, N. A., & Jones, P. D. (2012). Quantifying uncertainties in global and regional temperature change using an ensemble of observational estimates: The HadCRUT4 data set. *Journal of Geophysical Research*, *117*, D08101. https://doi.org/10.1029/2011JD017187

Myhre, G., Samset, B. H., Schulz, M., Balkanski, Y., Bauer, S., Berntsen, T. K., et al. (2013). Radiative forcing of the direct aerosol effect from AeroCom Phase II simulations. *Atmospheric Chemistry and Physics*, *13*, 1853–1877.

Rogelj, J., Elzen, M. D., Höhne, N., Fransen, T., Fekete, H., Winkler, H., et al. (2016). Paris Agreement climate proposals need a boost to keep warming well below 2°C. *Nature*, *534*, 631–639.

Schurer, A. P., Mann, M. E., Hawkins, E., Tett, S. F. B., & Hegerl, G. C. (2017). Importance of the pre-industrial baseline for likelihood of exceeding Paris goals. *Nature Climate Change*, *7*, 563–567.

Shindell, D. T. (2014). Inhomogeneous forcing and transient climate sensitivity. *Nature Climate Change*, *4*, 274–277.

Shine, K. P., Fuglestvedt, J. S., Hailemariam, K., & Stuber, N. (2005). Alternatives to the global warming potential for comparing climate impacts of emissions of greenhouse gases. *Climatic Change*, *68*(3), 281–302.

Solomon, S., Plattner, G. K., Knutti, R., & Friedlingstein, P. (2009). Irreversible climate change due to carbon dioxide emissions. *PNAS*, *106*(6), 1704–1709.

Stocker, T. F., Qin, D., Plattner, G. K., Tignor, M., Allen, S. K., Boschung, J., et al. (2013). IPCC AR5: Summary for policymakers, *Climate change 2013: The physical science basis. Contribution of Working Group I to the Fifth Assessment Report of the Intergovernmental Panel on Climate Change*. Cambridge, United Kingdom and New York, NY, USA: Cambridge University Press.

United Nations Framework Convention on Climate Change (2015). Adoption of the Paris Agreement FCCC/CP/2015/L.9/Rev.1.

Wigley, T. M. L. (1998). The Kyoto protocol: CO_2, CH4, and climate implications. *Geophysical Research Letters*, *25*(13), 2285–2288.

Zickfeld, K., Ebya, M., Matthews, H. D., & Weavera, A. J. (2009). Setting cumulative emissions targets to reduce the risk of dangerous climate change. *PNAS*, *106*(38), 16,129–16,134.